

SYNTHESIS AND CHARACTERIZATION OF CALCIUM PHOSPHATE AND ITS RELATION TO CR(VI) ADSORPTION PROPERTIES

Francisco GRANADOS-CORREA*, Juan BONIFACIO-MARTÍNEZ and Juan SERRANO-GÓMEZ

Depto. de Química, Instituto Nacional de Investigaciones Nucleares, A. P. 18-1027. Col. Escandón. Delegación Miguel Hidalgo. C. P. 11901. México, D. F., México. *Correo electrónico: francisco.granados@inin.gob.mx.

(Recibido junio 2008, aceptado septiembre 2009)

Key words: calcium phosphate, synthesis, characterization, Cr(VI) adsorption, surface area, adsorption experiments

ABSTRACT

Calcium phosphate with hydroxyapatite structure was synthesized and its ability to adsorb Cr(VI) from aqueous solution is presented. XRD, BET, IR, TGA, SEM and EDS techniques were used to characterize the obtained material. A pure phase was obtained through a simple synthesis process. The specific surface area of the synthesized powder was found to be $64.5 \text{ m}^2 \text{ g}^{-1}$. The X-ray diffraction pattern shows that the calcium phosphate formed was nanocrystalline with an average grain size of approximately 75 nm. A fast adsorption was observed and in less than 24 h it was found that $2.41 \times 10^{-4} \text{ meq g}^{-1}$ of Cr(VI) ions were adsorbed on calcium phosphate. Desorption experiments showed that Cr(VI) adsorption decreased to $2.23 \times 10^{-4} \text{ meq g}^{-1}$ of calcium phosphate. This behavior is a consequence of partial dehydration of the synthesized material. Calcium phosphate can be effectively used for removing Cr(VI) from aqueous solutions in treatment processes of metal wastes.

Palabras clave: fosfato de calcio, síntesis, caracterización, adsorción de Cr(VI), área superficial, experimentos de adsorción

RESUMEN

Se sintetizó fosfato de calcio, con la estructura de la hidroxiapatita, y se presenta su habilidad para adsorber Cr(VI) en solución acuosa. Para caracterizar el material obtenido se usaron técnicas de DRX, BET, IR, ATG, MEB y EDS. Se obtuvo una fase pura por un proceso simple de síntesis. El área específica del polvo sintetizado fue de $64.5 \text{ m}^2 \text{ g}^{-1}$. El patrón de difracción de rayos-X muestra que el fosfato de calcio formado fue nanocristalino con un promedio de grano alrededor de 75 nm. Se observó una rápida adsorción en menos de 24 h y se encontró que $2.41 \times 10^{-4} \text{ meq g}^{-1}$ de iones Cr(VI) fueron adsorbidos sobre el fosfato de calcio. Experimentos de desadsorción mostraron que la adsorción de Cr(VI) disminuyó a $2.23 \times 10^{-4} \text{ meq g}^{-1}$ de fosfato de calcio. Este comportamiento es una consecuencia de la deshidratación parcial del material sintetizado. El fosfato de calcio puede ser usado efectivamente para la remoción de Cr(VI) de soluciones acuosas en los procesos de tratamiento de desechos de metales.

INTRODUCTION

During the last decade, obtaining porous materials for applications in many fields of technology has shown great development. Calcium phosphate with apatite structure ($\text{Ca}_{10}(\text{PO}_4)_6(\text{OH})_2$) is a sparingly soluble mineral with strong affinity for adsorption of radio nuclides and heavy metals. It has been proposed for use as a backfill material for geologic repositories for nuclear waste (Qureshi and Varshney 1991), and as an adsorbent in engineered barrier for environmental restoration (Ewing 2002). Additionally, it shows promise for other potential applications such as acidic or basic catalysts, chromatographic adsorbent and as biomaterial (Matsuda *et al.* 2005, Thakur *et al.* 2005).

In particular, the use of calcium phosphate as an adsorbent is due to its large specific area, high thermal and chemical stability, high ionic exchange capacity and its stability towards ionizing radiation. Therefore, its characteristics resulting from the preparation method exert an important influence on its behavior as inorganic exchanger to remove contaminants present in water. In many researches, various types of phosphates, such as acid metal phosphates of zirconium, aluminum, titanium and tin, have been synthesized for use as ionic exchangers (Qureshi and Varshney 1991, El-Said *et al.* 2001, Da-Rocha *et al.* 2002).

Various methods to synthesize calcium phosphate have been reported (Yoshida 1996, Ayres *et al.* 1998, Andronescu *et al.* 2002), where calcium is supplied as aqueous solutions of CaCl_2 , $\text{Ca}(\text{NO}_3)_2$, CaCO_3 or $\text{Ca}(\text{CH}_3\text{COO})_2$ and phosphates are supplied as aqueous solutions of $(\text{NH}_2)\text{HPO}_4$, $\text{NH}_4\text{H}_2\text{PO}_4$, KH_2PO_4 , N_2HPO_4 , or NaH_2PO_4 .

In this work, calcium phosphate was synthesized by using the continuous precipitation method, and its structural and surface characteristics were determined to test the adsorption of Cr(VI) ions present in aqueous solution.

MATERIAL AND METHODS

Materials

Calcium phosphate was synthesized at room temperature by the continuous precipitation method as reported by Gómez-Morales *et al.* (2001). To obtain 10 g of calcium phosphate (hydroxyapatite) 23.51 g calcium nitrate tetrahydrate $\text{Ca}(\text{NO}_3)_2 \cdot 4\text{H}_2\text{O}$ A.C.S. reagent (Sigma-Aldrich, 99 wt% purity) and 6.87 g monobasic ammonium dihydrogen-phosphate (NH_4

H_2PO_4 A.C.S. reagent (Sigma-Aldrich, 98 wt% purity) were used. The reagents were mixed at a Ca/P molar ratio of 1.67. K_2CrO_4 (Baker) was used for the adsorption experiments.

Synthesis by continuous precipitation

Calcium phosphate was prepared with 23.51 g of $\text{Ca}(\text{NO}_3)_2 \cdot 4\text{H}_2\text{O}$, dissolved in 545 mL distilled water with an initial pH of 5. Later, this solution was mixed with 62 mL of concentrated NH_4OH ; the final pH of the solution obtained was 12. Finally, distilled water was poured into the beaker to attain a total volume of 890 mL. The same purity criteria were used to prepare aqueous solution of monobasic ammonium phosphate: 6.9 g of $\text{NH}_4\text{H}_2\text{PO}_4$ were dissolved in 833 mL of distilled water with a pH value of 5. Then, 37 mL of concentrated NH_4OH were added to reach a pH value of 12. Finally, the obtained solution was diluted with distilled water up to a volume of 1500 mL. To obtain calcium phosphate, ammonium phosphate solution was slowly poured into calcium nitrate solution under vigorous stirring for 24 h. The suspension was left to settle for another 24 h, to finally draw off the supernatant. The precipitate was washed four times with distilled water under stirring for 18 h and then the solid and liquid phases were separated by centrifuging. The calcium phosphate obtained was dried at 120 °C for 2.5 hours and calcined at 1050 °C for 2.5 hours more. This thermal treatment made calcium phosphate more crystalline and destroyed and volatilized the nitrate and ammonium traces trapped in the solid.

Characterization

Specific surface of calcium phosphate was obtained by nitrogen adsorption through the BET method with a surface area analyzer Micromeritics Gemini 2360. The solid sample was heated for 2 h at 200 °C. Infrared measurements were performed using a Nicolet 550 spectrophotometer and the sample was mixed with KBr in the conventional way. A Siemens D500 diffractometer coupled to a copper anode tube was used to obtain the X-ray diffraction patterns and identify the crystalline compounds. The K_α wavelength was selected with a diffracted beam monochromator. The X-ray tube was operated at 35 kV and 20 mA. All diffraction patterns were obtained in scanning mode with a 0.02° (2θ) step size. Crystalline calcium phosphate (hydroxyapatite) was identified conventionally with the JCPDS files.

The thermogravimetric analysis (TGA) were carried out with a TA Instrument TGA-51 under a flowing nitrogen atmosphere in a heating condition

of $10\text{ }^\circ\text{K min}^{-1}$; 15.0 mg samples and high purity N_2 gas were used.

Topography and morphology of the synthesized material were determined using a scanning electron microscopy (SEM; JOEL JSM-5900 LV) with an accelerating voltage of 30 keV and a maximum magnification of 1000X. Semi-quantitative analysis of the selected micro area of calcium phosphate (hydroxyapatite) samples were carried out by energy dispersive X-ray analysis (EDS) technique using Oxford microprobe coupled to the electronic microscope.

Chromium adsorption

Batch experiments were carried out at room temperature mixing in closed vials, 0.1 g of calcium phosphate and 10 mL of 1.0×10^{-4} M Cr(VI) solution at pH 5.5. Samples were stirred for 10 s and shaken for 48 h. The liquids were separated from the solids by centrifuging (5 min at 3000 rpm). Chromium concentrations in each aliquot of 5 mL solutions was determined by using a Shimadzu ultraviolet-visible 265 spectrophotometer analyzer at $\lambda=540$ nm using the 1,5 diphenylcarbazide method. Efficiency of Cr(VI) adsorption on calcium phosphate was determined in milliequivalents of ion adsorbed per gram of solid. The Cr(VI) adsorption by calcium phosphate could be explained by physical adsorption and as this process is reversible, physical adsorption was estimated by desorption experiments. The best Cr(VI) exchanged sample was suspended in deionized water and chromium content in the aqueous phase was measured as a function of time, until an equilibrium was reached between the sample and the aqueous phase.

RESULTS AND DISCUSSION

The specific area of the synthesized material was found to be $64.5\text{ m}^2\text{ g}^{-1}$; a value which coincides with data reported by Yoshida (1996) for calcium phosphate type hydroxyapatite. The infrared spectrum of calcium phosphate is shown in **figure 1**. The bands at $\nu_1 = 962.6$ and $\nu_2 = 1040\text{ cm}^{-1}$ are assigned to the fundamental frequencies of the PO_4^{3-} group. A low intensity band can be observed at 957 cm^{-1} which is assigned to the vibration of the P-OH group. The broad band at 3192 cm^{-1} results from an overlapping of hydrogen vibrations: stretching vibrations of structural OH^- and physically adsorbed water. The low intensity band at 1630 cm^{-1} is assigned to bending vibrations of strongly adsorbed water. The band observed at 1432 cm^{-1} is very probably due to the presence of a very small amount of

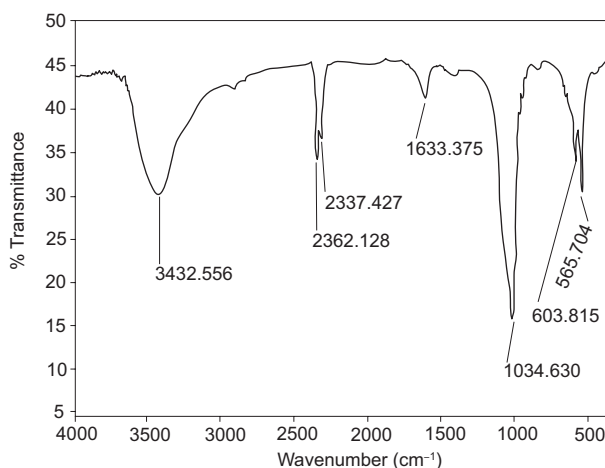


Fig. 1. IR spectrum of calcium phosphate

calcium carbonate. To lower frequencies, two bands assigned to the PO_4^{3-} ion can be found: the intense band at 1032 cm^{-1} (ν_3) and the low intensity band at 567 cm^{-1} (ν_4). Thus, the IR spectrum in figure 1 indicates the high purity of the analyzed calcium phosphate (hydroxyapatite).

Figure 2 shows the XRD pattern of the obtained powders: the examination of the figure indicates that the synthesized material was only a crystalline single phase. The indexation calculations reveal that this synthesized material has a hexagonal hydroxyapatite structure with unit cell parameters calculated from the XRD patterns of $\text{Ca}_{10}(\text{PO}_4)_6(\text{OH})_2$ ($a=b=9.385\text{ \AA}$ and $c=6.870\text{ \AA}$) obtained from the procedure described by Suryanarayana *et al.* (1998), in strong agreement with literature data (Da-Rocha *et al.* 2002). According to Sherrer equation, the calcium phosphate formed was all nanocrystalline with an average grain size of about 75 nm. The most intense and sharp lines are observed

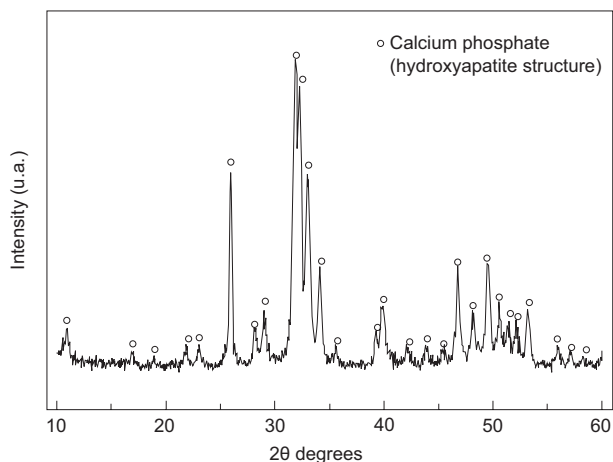


Fig. 2. XRD pattern of calcium phosphate

in the 2θ angle range between 20 and 60° . These lines are coincident with the lines of the XRD spectrum reported in JCPDS 9-0432 file, which corresponds to hydroxyapatite. The XRD pattern in **figure 2** shows that water detected by IR spectroscopy in the calcium phosphate sample does not alter the structure of this material.

The thermogravimetric analysis (TGA) results of the synthesized calcium phosphate (hydroxyapatite) are shown in **figure 3**. The TGA curves display a continuous slow mass loss with a constant temperature increase. In the derivative curve the peak observed at about 43°C indicates a relatively slow moisture loss at an almost constant rate. At about 150°C there is a small slope change in the TGA curve, indicating a different type of mass loss, which is that of strongly adsorbed water whose loss rate is rather low and can be seen in the derivative curve as a non-intense and small peak which ends at about 325°C . The water molecules were lost as calcium phosphate was increasingly heated. A fast slope change of the TGA curve is presented over the 300°C with a maximum at about 325°C in the derivative curve, indicating again a mass loss which can be due to the dehydroxylation of the hydroxyapatite sample. A small peak at about 360°C is also observed in the derivative curve and it may be due to the decomposition of the carbonate ions detected by IR spectroscopy in the solid simple. These carbonate ions were formed as a result of CO_2 absorbed by the calcium phosphate. Finally, another fast change in the TGA curve can be seen at about 600°C and the mass loss in this case may be due to phosphate ion decomposition observed as the two peaks displayed at 642 and 697°C . These results show that the calcium phosphate is stable at temperatures below 600°C .

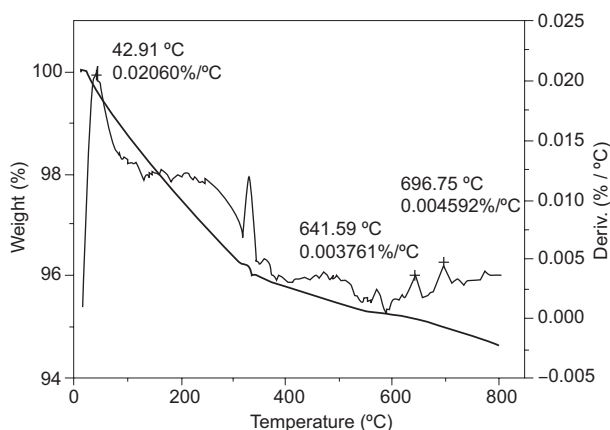


Fig. 3. Thermogravimetric analysis of calcium phosphate

Figure 4 shows the micrograph of hydroxyapatite obtained by SEM. The material has a particle size range of $5\text{--}40\ \mu\text{m}$, indicating a high dispersion in particle size. The graphic results of the semiquantitative elemental chemical analysis yielded by EDS technique shows that the elemental composition of the final synthesized white powders were found to be P 27.47 wt%, Ca 19.64 wt% and O 52.89 wt%. These results reveal high purity of the calcium phosphate obtained by the continuous precipitation method since no other chemical element was detected by the EDS technique when hydroxyapatite was analyzed in different zones of the sample.

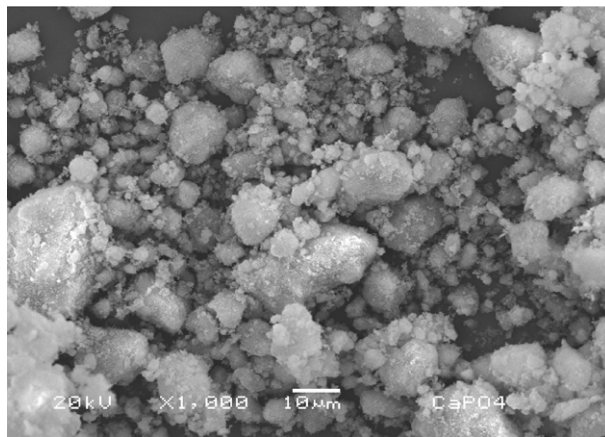


Fig. 4. Micrograph and elemental microanalysis X-ray spectrum of calcium phosphate

The amount of chromium ions retained on calcium phosphate is shown in **figure 5**. At first, a fast Cr(VI) adsorption on calcium phosphate was observed and at 24 h of contact time, a maximum adsorption was found to be 2.41×10^{-4} meq Cr(VI) g^{-1} . Cr(VI) adsorption data as a function of the adsorbate concentration were examined in terms of the Freundlich adsorption model. In **figure 6** the logarithm of the amount adsorbed ($\log a_e$) of Cr(VI) at equilibrium has been plotted versus logarithm of Cr(VI) concentration ($\log C_e$) in solution at equilibrium at pH 5.5. The obtained straight line in **figure 6** shows that Cr(VI) adsorption data fit well with the Freundlich isotherm in its logarithmic form:

$$\text{Log } q_e = 1/n \text{ log } C_e + \text{Log } K \quad (1)$$

K and $1/n$ ($0 < 1/n < 1$) being Freundlich constants which refer to the adsorption capacity and intensity of adsorption. The values of these constants can be

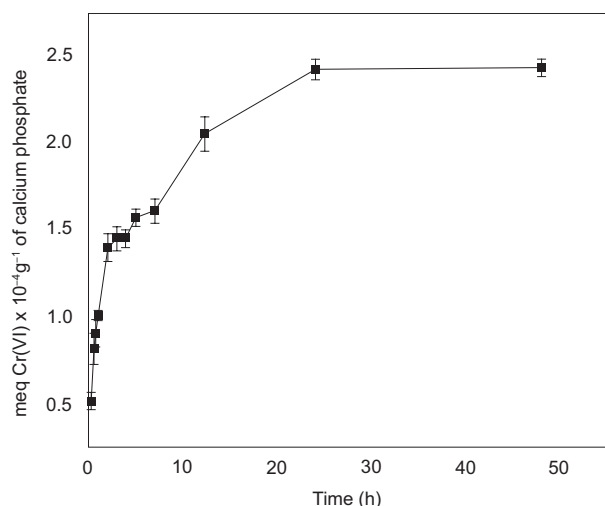


Fig. 5. Milliequivalents of Cr(VI) per gram of calcium phosphate, pH 5.5 and room temperature

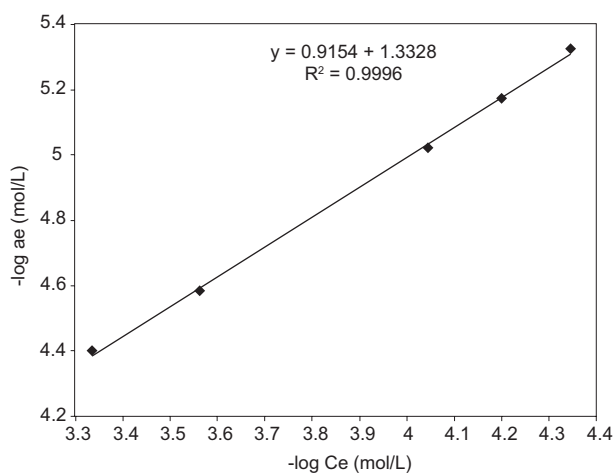


Fig. 6. Freundlich adsorption isotherm for Cr(VI) ions adsorption on calcium phosphate

estimated by the intercept and the slope (less than 1) of the straight line, respectively. The values of K and $1/n$, computed by using the least squares technique, were found to be $0.0464 \text{ mol g}^{-1}$ and $0.9154 \text{ mol g}^{-1}$ respectively, with a correlation factor of 0.9996. The value of $1/n$ (less than one) found in this work confirm that the Freundlich isotherm is valid for the Cr(VI) adsorption data and this suggest that the adsorbent surface is heterogeneous in nature with an exponential distribution of the active centers.

Figure 7 presents the desorption of Cr(VI) from calcium phosphate; as can be seen, a minimum amount of desorbed chromium before 3 h in water was observed. When the calcium phosphate was left in water for a longer time, 12 h, no more chromium was left in solution indicating that equilibrium had

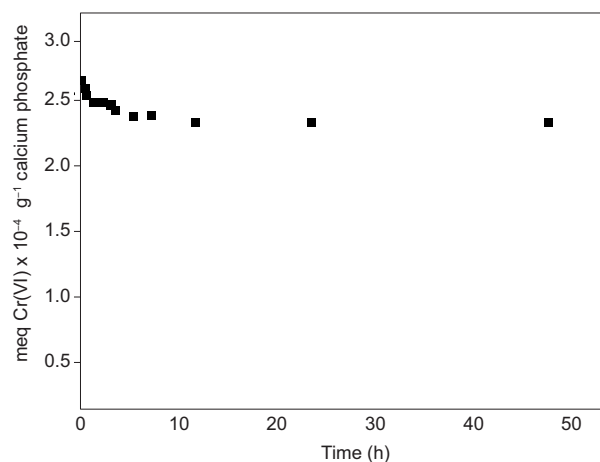


Fig. 7. Cr(VI) desorption in water from calcium phosphate

been reached. Then, the chromium ion desorption was minimum and indicates that physical adsorption in the surface of calcium phosphate did not considerably contribute during adsorption. **Figure 7** shows that after the desorption process, the final adsorption capacity at equilibrium was $2.23 \times 10^{-4} \text{ meq Cr(VI) g}^{-1}$ of calcium phosphate, a value very close to that obtained by the Cr(VI) adsorption.

The specific surface area of a solid material is related to a number of surface active sites available to retain the chemical species to be removed from the contaminated aqueous solution. Therefore, calcium phosphate synthesized in our laboratories has a good adsorption behavior of Cr(VI) species because of its specific surface area is high: $64.5 \text{ m}^2 \text{ g}^{-1}$. The X-ray diffraction pattern showed that the calcium phosphate formed was nanocrystalline with an average grain size of 75 nm. This grain size can not be considered small and to reduce it by fragmentation to much smaller values can improve the adsorption behavior of the calcium phosphate because a material with a higher specific area will be obtained. On the other hand, the high purity of calcium phosphate (as revealed by the corresponding IR spectrum and EDS analysis) and the value of the maximum Cr(VI) adsorption found in this work show that a pure material is required to obtain optimum Cr(VI) removal results.

CONCLUSIONS

Pure and crystallized calcium phosphate powders with hydroxyapatite structure was synthesized by continuous precipitation method using $\text{Ca}(\text{NO}_3)_2 \cdot 4\text{H}_2\text{O}$ and $\text{NH}_4\text{H}_2\text{PO}_4$. This procedure allows obtaining a material with a specific chemical

composition and controlled powder morphology, both of which are essential for the application of hydroxyapatite as an adsorbent. The maximum sorption of Cr(VI) was found to be 2.41×10^{-4} meq Cr(VI) g^{-1} of calcium phosphate. In desorption experiments the chromium ion desorption was minimum, and thus a high selectivity was found for chromium for the exchange process in this calcium phosphate. Therefore the obtained inorganic material presents an optimal surface and structural properties to be used as an adsorbent material in the removal of Cr(VI) present in aqueous wastes.

ACKNOWLEDGEMENTS

The authors thank to the Consejo Nacional de Ciencia y Tecnología (CONACyT, México) project 52858-II and project ININ-CB-718, for financial support.

REFERENCES

- Qureshi M. and Varshney K.G. (1991). *Inorganic ion exchangers in chemical analysis*. CRC Press, Boca Raton Florida, USA, 282 pp.
- Andronescu E., Stefan E., Dinu E. and Ghitulica C. (2002). Hydroxyapatite synthesis. *Eur. Ceram.* 206, 1595-1598.
- Ayers R., Simske S., Nunes C. and Woford L. (1998). Long-term bone in growth and residual microhardness of porous block hydroxyapatite implants in human. *J. Oral Maxil. Surg.* 56, 297-1301.
- Da-Rocha N.C., De Campos R.C., Rossi A.M., Moreira E.L., Barbosa A. F. and Moure G.T. (2002). Cadmium uptake by hydroxyapatite synthesized in different conditions and submitted to thermal treatment. *Environ. Sci. Technol.* 36, 1630-1635.
- El-Said N., Siliman A.M., El-Sherif E. and Mikhail, A.S. (2001). Separation and speciation of fission products by zirconium phosphate prepared by solid-solid reaction. *Radiochim. Acta* 89, 647-652.
- Ewing R.C. (2001). The design and evaluation of nuclear-waste forms: clues from mineralogy. *Can. Mineral.* 39, 697-715.
- Gómez-Morales J., Torrent-Burgués J., Boix T., Fraile J. and Rodríguez-Clemente R. (2001). Precipitation of stoichiometric hydroxyapatite by a continuous method. *Cryst. Res. Technol.* 36, 15-26.
- Matsuda T., Yamanaka C. and Ikeda M. (2005). ESR study of Gd^{3+} and Mn^{2+} ions sorbed on hydroxyapatite. *Appl. Radiat. Isotopes* 62, 353-357.
- Suryanarayana C. and Norton M.G. (1998). *X-ray diffraction. A practical approach*. Plenum Press, New York, USA, 273 p.
- Thakur P., Moore R.C. and Chopin G.R. (2005). Sorption of U(VI) species on hydroxyapatite. *Radiochim. Acta* 93, 385-391.
- Yoshida K. (1996). Osteoinduction capability of recombinant human bone morphogenetic protein-2 in intramuscular and subcutaneous sites: an experimental study. *J. Cranio. Maxill. Surg.* 26, 112-115.